

Phase rotation for the muon collider

R.C. Fernow
Brookhaven National Laboratory

12 November 2004

We survey previous designs for single-bunch phase rotation for the muon collider. The performance of each of the designs is simulated using the same initial beam distribution, the same radial constraints, and the same simulation code (ICOOL). The 36 MHz design of V. Balbekov gave the best performance. A more realistic simulation was performed on a 40 MHz design of the same type. The realistic simulation included the tapered wall, extended rf cavities, windows and periodic solenoid channel. We obtained $0.47 \mu/p$ into a 6 m bunch with $200 < p < 400$ MeV/c. Reducing the initial target bunch length from 3 ns to 1 ns increased the yield by an additional 13%.

1. Introduction

At the moment no complete design exists for the front end of a muon collider. However, one of the most promising approaches is to capture a single bunch of pions shortly following the production target. Designs of this type have been presented in the 1996 Snowmass report [1], the 1999 status report [2], and in a more recent technical note by V. Balbekov [3]. In addition two of the neutrino factory designs have low-frequency rf near the target and might also be useful for a muon collider, i.e. the beginning of the PJK [4] and CERN [5] channels. Each of these designs was originally simulated using different initial particle distributions, different radial cuts and with different simulation codes. Our first goal here is to compare the performance of each of these designs by reexamining them under identical conditions. We use an initial particle distribution obtained from the interaction of 24 GeV protons on mercury in MARS. The proton driver bunch length was 3.2 ns. This is the same distribution used in Study 2a for the neutrino factory. All of the simulations were performed using version 2.77 of ICOOL.

A number of simplifications were used in the simulations for the initial survey of the designs. We tried to reproduce the original published designs as faithfully as possible. We then looked at variations in the design parameters to optimize the performance. The strategy was to select the best of these initial designs as the candidate for further detailed studies in more realistic simulations.

The performance of a phase rotation channel is strongly affected by the field gradient assumed for the cavities. There is a wide difference of opinion on what is a reasonable gradient to assume for these low-frequency room-temperature rf cavities. Table 1 shows the gradients assumed for the simulations mentioned above

Table 1: Summary of gradients used in phase rotation simulations.

f	G	ref
MHz	MV/m	
5	0.2	PRISM
30	2.1	Snow
	4	SR
	5	PJK
36.37	6.37	VB
37	4	SR
44	2	CERN
45	7	PJK
50	3.3	Snow
60	3.6	Snow
	5	SR
	8	PJK
88	4	CERN
90	4.2	Snow
	18	SR
100	4.5	Snow

2. Survey of single-bunch phase rotator designs

Each design used a solenoidal capture field that started at 20 T at the target and fell off to an asymptotic field B_1 after a distance L_{TAP} . The fall-off of the field was assumed to have the same functional dependence used in Study 2 of the U.S. neutrino factory. We used an optimization program to find a set of current sheets that reproduced the desired magnetic field on-axis. Once the field reached B_1 , the remainder of the channel used a constant solenoidal field. The rf cavities were modeled as 2 cm parallel plates with fields varying sinusoidally with time at the center of a 1 m long region. A very large gradient was used, such that the average gradient over the 1 m had the specified value. The beam pipe had a constant radial cut-off of 30 cm. A more realistic simulation is given in section 3.

For the initial survey we use as a figure of merit the total number of particles in a selected momentum band at the end of the channel. We examine the transmission in two momentum bands: $100 < p < 300$ MeV/c, which is centered on the acceptance of many cooling channels, and for comparison $200 < p < 400$ MeV/c, which is slightly higher than what is normally used. The higher momentum phase rotator could be followed by a mini-cooling stage to bring the momentum back to the optimal value for a cooling channel.

Performance results for all the designs are summarized in section 2.6. The reference momentum or cavity phase shift was tuned for each channel to give optimum performance. The dependence of the transmission on these and other parameters is shown in detail for the Balbekov model in section 2.5.

2.1 Snowmass design

The Snowmass report [1] contained two phase rotation designs. The high energy solution was designed to capture pions with kinetic energy 200-700 MeV. This energy is high compared to the operating range for conventional ionization cooling channels and rings, so we do not consider this solution any further. The layout of the low energy phase rotator is shown in Fig. 1.

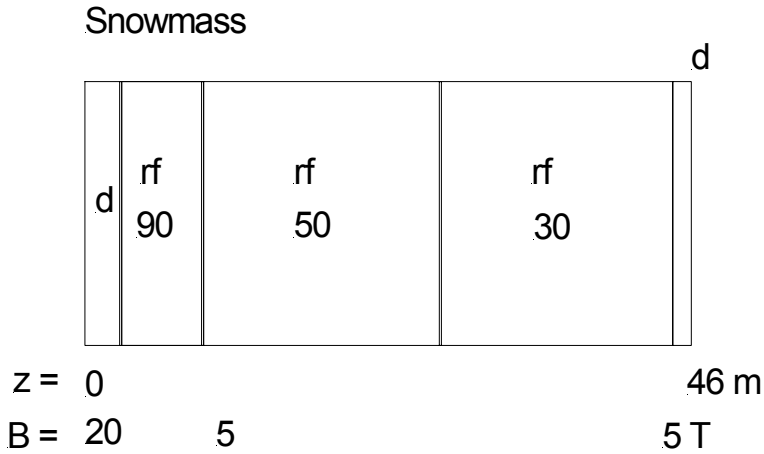


Figure 1. Layout of the low-energy Snowmass phase rotation model.

We assume the fields falls to 5 T over a distance of 9 m. We assume the rf begins 3 m downstream of the target. There are cavities with three different rf frequencies spread out over 42 m. The longitudinal phase space at the end of the channel is shown in Fig. 2.

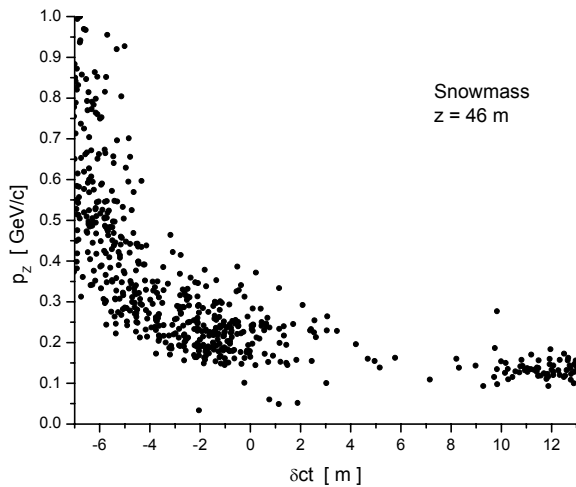


Figure 2. Longitudinal phase space at the end of the Snowmass phase rotation channel.

The total transmission into the lower momentum band was 35%.

2.2 Status report design

The status report [2] contains similar, but not identical, low and high energy phase rotation designs to those given in the Snowmass report. The layout of the low energy phase rotator is shown in Fig. 3.

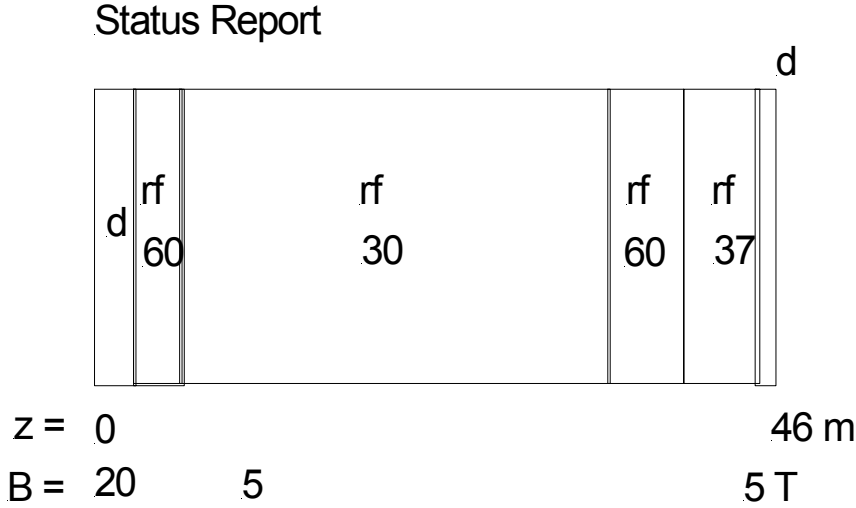


Figure 3. Layout of the low-energy status report phase rotation model.

We assume the fields falls to 5 T over a distance of 9 m. We assume the rf begins 3 m downstream of the target. There are cavities with three different rf frequencies spread out over 42 m. The longitudinal phase space at the end of the channel is shown in Fig. 4.

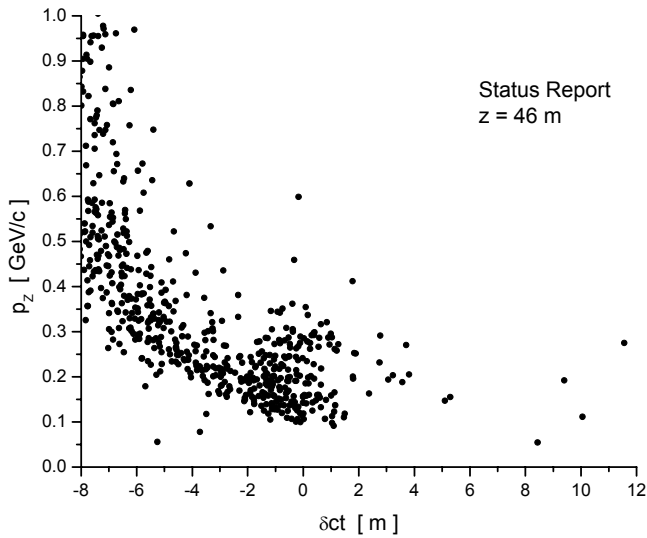


Figure 4. Longitudinal phase space at the end of the status report phase rotation channel.

The total transmission into the lower momentum band was 34%.

2.3 CERN neutrino factory design

The CERN neutrino factory [5] begins with a 44 MHz channel 30 m downstream from the target. The design gradient was 2 MV/m. We substitute a 20 T solenoid for the horn that CERN uses for the pion collection around the target. The layout is shown in Fig. 5.

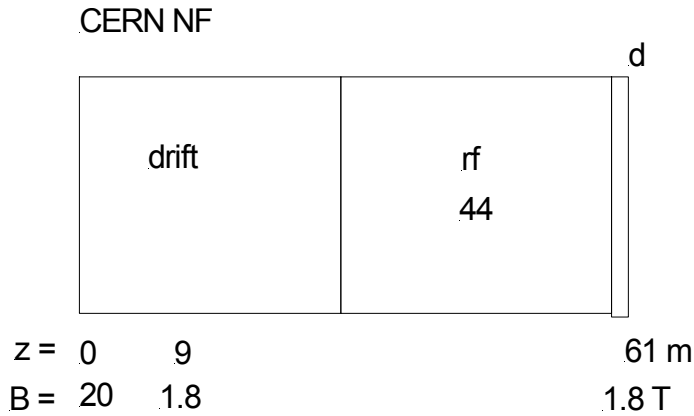


Figure 5. Layout of the CERN neutrino factory phase rotation model.

We assume the field falls to 1.75 T over a distance of 9 m. CERN used 1.8 T for the channel field. There is just one frequency of rf spread out over 30 m. The longitudinal phase space at the end of the channel is shown in Fig. 6.

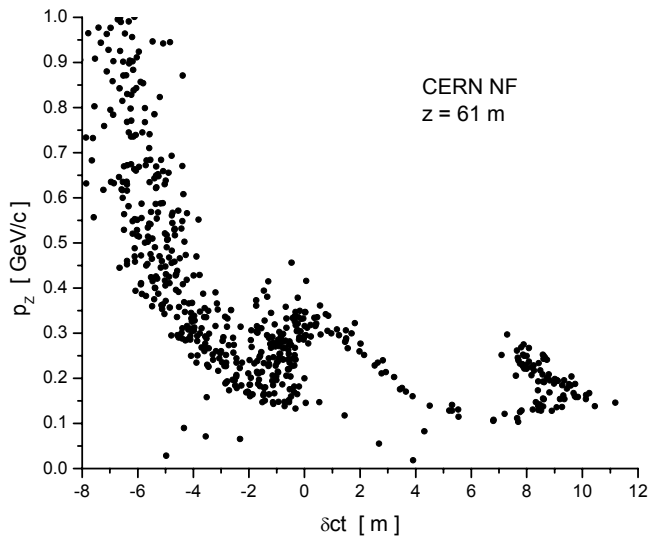


Figure 6. Longitudinal phase space at the end of the CERN phase rotation channel.

The total transmission into the lower momentum band was 30%. This result only improved slightly with a 4 MV/m gradient.

2.4 PJK design

The rf cavities in the PJK neutrino factory design [4] begin 3 m downstream of the target. The layout is shown in Fig. 7.

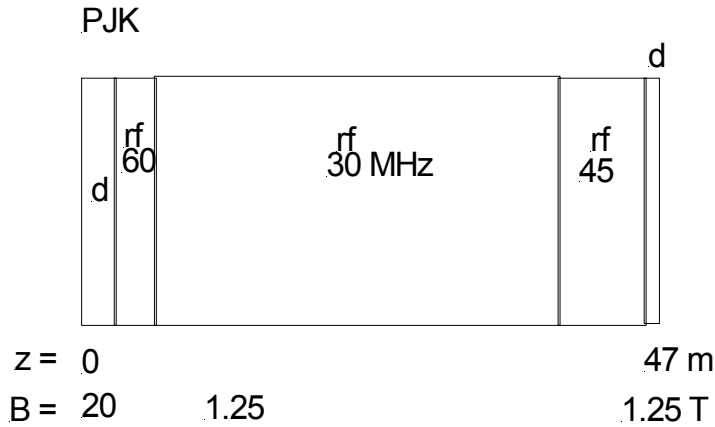


Figure 7. Layout of the PJK neutrino factory phase rotation model.

We assume the field falls to 1.25 T over a distance of 9 m. There are three different rf frequencies spread out over 43 m. The longitudinal phase space at the end of the channel is shown in Fig. 8.

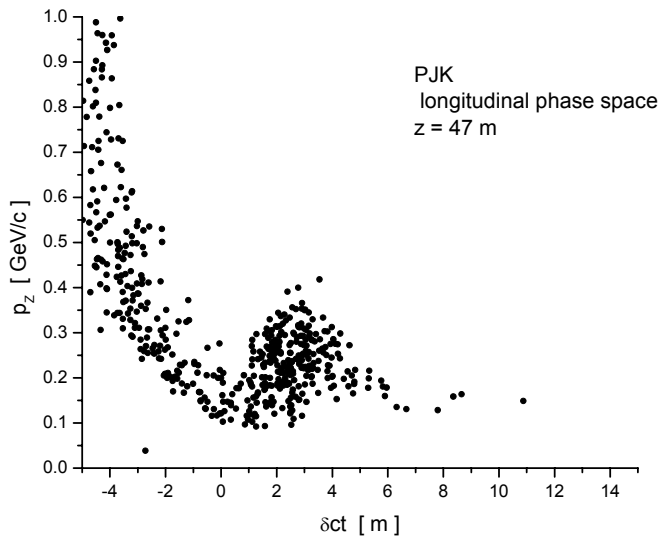


Figure 8. Longitudinal phase space at the end of the PJK phase rotation channel.

The total transmission into the lower momentum band was 31%. The performance can be improved to 33% by increasing the solenoidal field in the channel to 1.75 T.

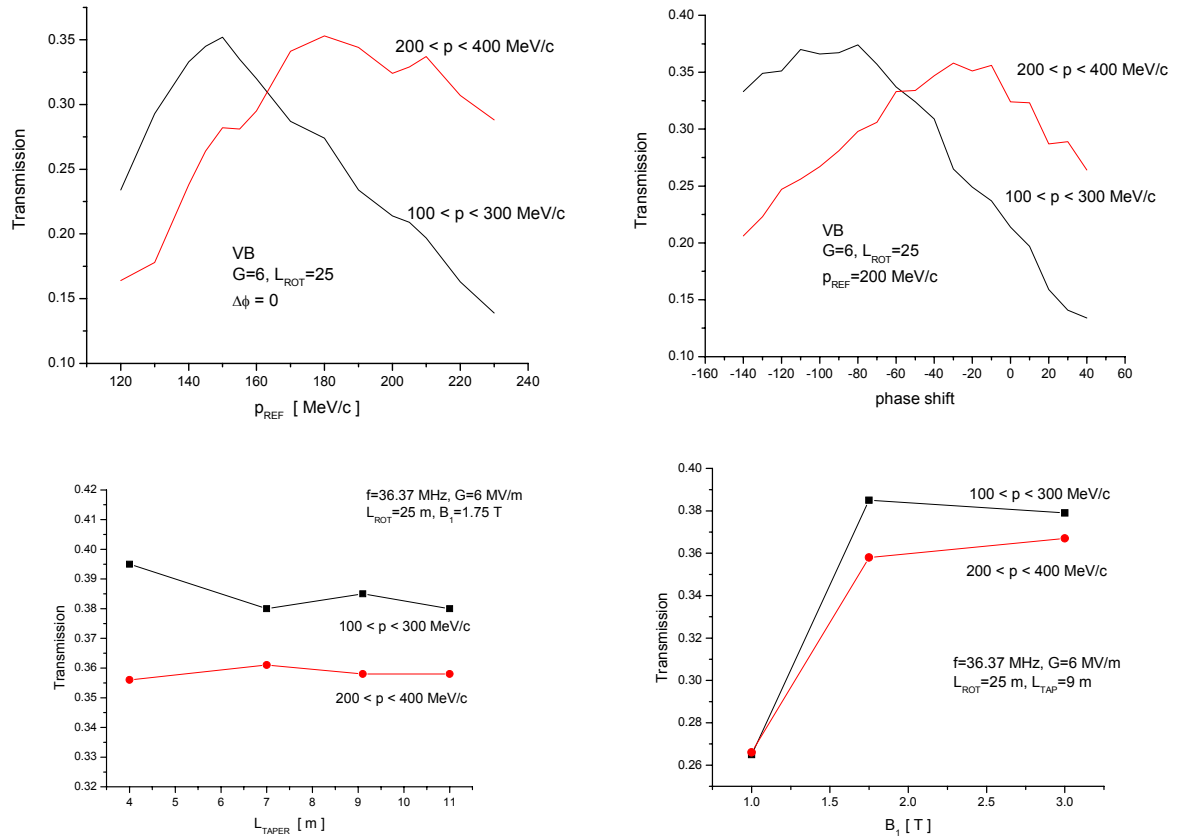


Figure 11. Dependence of the transmission into fixed momentum bands as a function of (a) reference momentum, (b) cavity phase shift, (c) length of the solenoid taper and (d) asymptotic field in the channel.

The cavity phase can be tuned either by changing the reference particle momentum or by adjusting the phase shift in the cavities. These methods give similar, but not identical results. There is a slight tendency for the transmission of the lower momentum band to fall with increasing length of the solenoidal field taper. For a fixed channel radius of 30 cm, there is significant loss until the asymptotic value of the solenoid field in the channel reaches the matched value of 1.75 T.

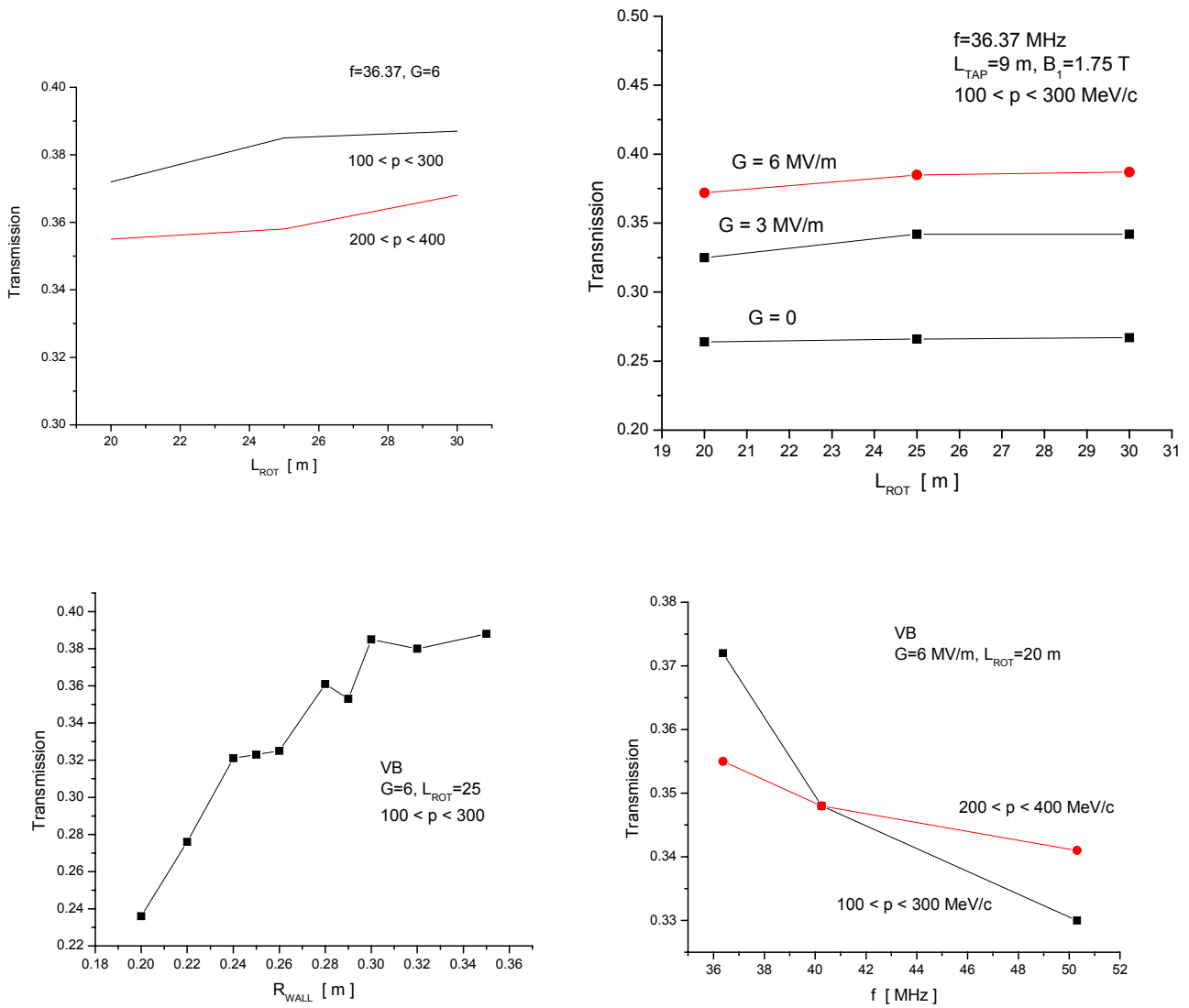


Figure 12. Dependence of the transmission into fixed momentum bands as a function of (a) length of the rf cavity region, (b) cavity gradient, (c) radial cut-off in the channel and (d) frequency.

There is a slight improvement with the 25 m long section of rf cavities. The transmission improves with higher gradients. The transmission is ~40% higher for 6 MV/m than the case with no rf present. The performance of the 1.75 T channel flattens out for wall radii bigger than the matched value of 30 cm. The peak transmission falls off slowly for higher frequency.

The longitudinal phase space at the end of the channel is shown in Fig. 13.

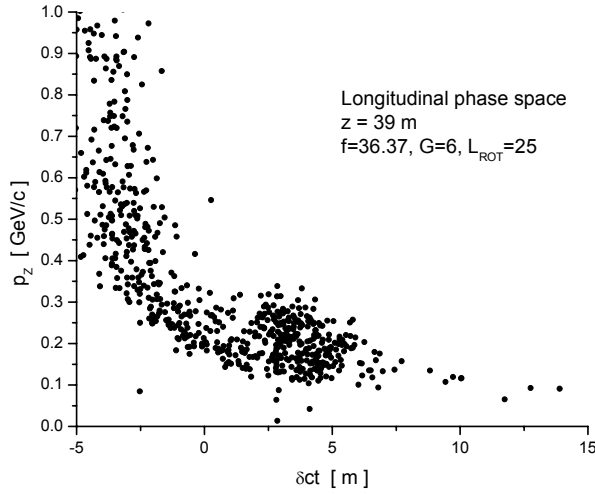


Figure 13. Longitudinal phase space at the end of the Balbekov phase rotation channel.

The total transmission into the lower momentum band was 38%.

2.6 Summary of survey results

Table 2 gives a summary of the survey results, including some variations from the basic designs. The transmission numbers in this table include a bunch length cut of 6 m. All these designs used a solenoidal field taper of 9 m.

Table 2: Summary of phase rotation performance results

	B_1	f	G	L_{ROT}	Tr	Tr
	[T]	[MHz]	[MV/m]	[m]	(100-300)	(200-400)
VB	1.75	36.37	6.37	20	0.277	0.334
	1.75	36.37	6	25	0.302	0.341
	1.75	40.25	6	25	0.303	0.344
PJK	1.25	60-30-45	8-5-7	43	0.257	0.277
	1.75	66-30-42	8-5-7	43	0.286	0.324
CERN	1.75	44	2	30	0.179	0.240
	1.75	44	4	30	0.180	0.258
SR	5	60-30-60-37	5-4-4-4	42	0.268	0.301
Snow	5	90-50-30	4.2-3.3-2.1	42	0.227	0.273

We see that the Balbekov design gives the best results. We choose the 40.25 MHz variation as our reference design for further study. This frequency is the 5th subharmonic of 201.25 MHz, which may be useful for subsequent parts of the front end.

3. Realistic phase rotation channel

The 40.25 MHz variation of the Balbekov design was the most promising candidate for the single-bunch phase rotator. The configuration is the same as discussed previously: a 4 m drift space, followed by a 25 m region containing rf, followed by a 10 m drift space. A number of features needed to be included to make a more realistic simulation:

- tapered wall
- Be window after target drift space
- extended rf cavity with pillbox fields
- periodic solenoid channel
- Be windows on the rf cavities

The radial cut-off due to the beam pipe is 10 cm at the target. This fits comfortably inside the 15 cm inner radius of the innermost copper coil, as shown below in Fig. 14. The radius tapers out to 30 cm over a distance of 4 m, following the scaling relation

$$r = \sqrt{\frac{\Phi}{\pi} \frac{1}{B(r)}}$$

where $\Phi/\pi = 1575 \text{ T cm}^2$ is the magnetic flux in the channel. We separate the mercury-filled target region from the rest of the channel by including a 2 mm thick Be window 4 m downstream from the target.

Since the radial extent of the 40 MHz cavity will be very large, no matter how it is constructed, it is impractical to put the solenoids radially outside the rf cavity. For a true pillbox the radius would be 2.85 m. Each longitudinal meter of the phase rotation channel must therefore be subdivided into space for the rf cavity, for the solenoid, and for clearance (drift). We assumed that 2 cm gaps are left between the rf cavities and the solenoids. Two competing effects determine the optimum length of the cavity. For a fixed gradient making the cavity longer gives more total voltage for phase rotation. On the other hand there is then less space available for the solenoid, the modulation of the field on-axis becomes larger, and losses due to momentum stop bands increase. We found the optimum distribution was 70 cm long cavities, which left 26 cm for the solenoids. This produced a solenoid field $1.75 \pm 0.43 \text{ T}$ on-axis.

The rf cavity is modeled as a cylindrical pill box. Each cavity is enclosed by two Be windows. The thickness of the window was determined from the scaling relation

$$t = 0.5 \text{ mm} \left(\frac{r}{21 \text{ cm}} \right)^4 \left(\frac{G}{16 \text{ MV/m}} \right)^2$$

For 30 cm radius and 6 MV/m gradient, this gives 300 μm thick rf windows.

The solenoids had an inner radius of 35 cm and a radial thickness of 15 cm. Once the axial location of the coils was determined, an optimization program was used to determine the current density in the solenoid coils. These coils were used to make a field map, so that subsequent optimization with ICOOL could proceed more quickly.

The coil configuration used for the simulation is shown in Fig. 14.

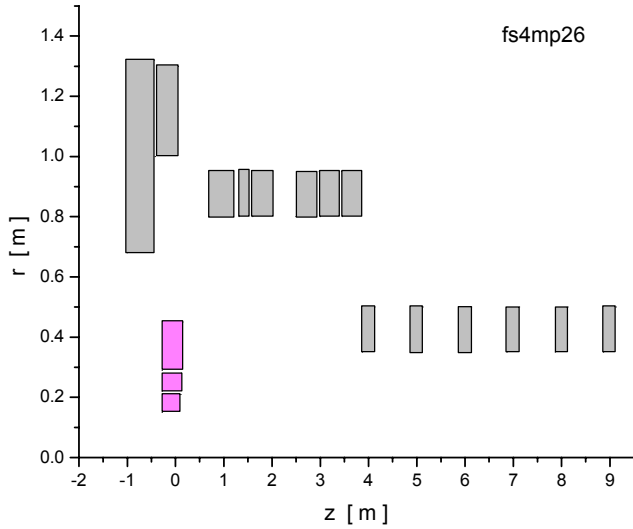


Figure 14. Configuration of solenoidal coils at the start of the phase rotation channel.

The rf cavities begin 4 m downstream from the end of the target. The coils in the taper region have been configured so that there is no interference with the low frequency rf cavities. The periodic decay channel also begins approximately 4 m from the target.

The layout of one cell of the rf region is shown in Fig. 15.

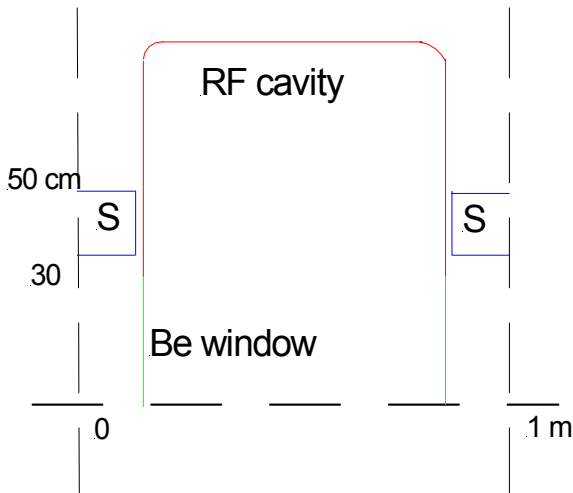


Figure 15. Layout of rf cells in the phase rotation channel.

The longitudinal phase space at the end of the realistic channel is shown in Fig. 16. In this example the phases of the rf cavities were set to maximize the number of particles in the momentum band $100 < p < 300$ MeV/c.

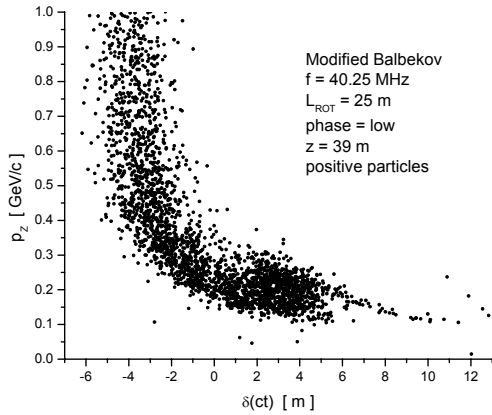


Figure 16. Longitudinal phase space at the end of the realistic phase rotation channel.

The number of μ/p in a 6 m long bunch with $100 < p < 300$ MeV/c is 0.39. If the cavity phases are readjusted, μ/p with $200 < p < 400$ MeV/c is 0.47. If the target bunch length is reduced from 3.2 to 1.0 ns, the yield in the low momentum band increases by 21% while the yield in the high momentum band increases by 13%.

When the proton beam hits the target positive and negative charged particle are produced simultaneously. The configuration described here does not separate the charges after the target, so particles of both signs enter the phase rotation channel. However, the rf phases have been adjusted for maximum performance with positive particles. Therefore, it is interesting to examine the characteristics of the negative beam at the end of the channel. The transmitted momentum distributions with the channel phases set for low momentum acceptance are shown in Fig. 17.

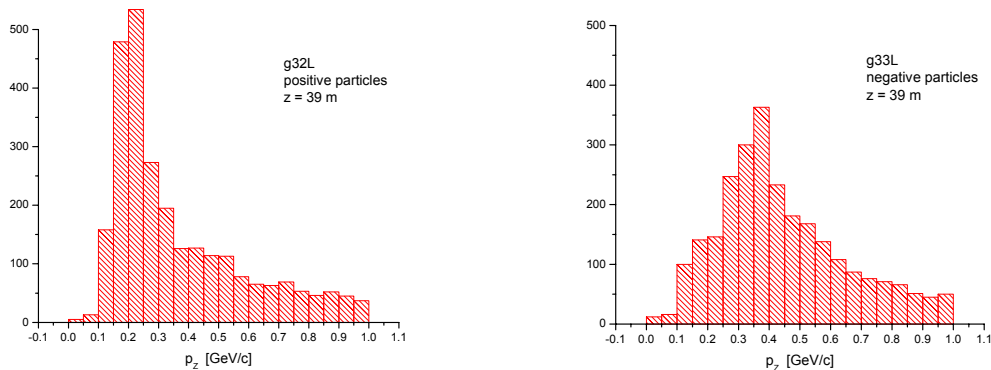


Figure 17. Momentum distributions of positive and negative particles at the end of the phase rotation channel.

The total number of transmitted negative particles is similar to the positives. However the negative momentum distribution is wider and centered at higher momenta. The final yields with a 6 m bunch length cut and a 3.2 ns proton driver pulse are summarized in Table 3.

Table 3. Muon yields at end of phase rotation system

case	sign	Δp [MeV/c]	μ / p
1	+	100 – 300	0.39
2	-	100 – 300	0.12
3	-	250 – 450	0.32
4	+	200 – 400	0.47
5	-	200 – 400	0.20
6	-	300 – 500	0.23

We also show the negative yield in a longitudinal phase space box of the same dimensions centered at the peak of the negative particle transmission. The negative yield for the low momentum band is 80% of the positive yield.

4. Prospects

The positive muon yields of 0.39 or 0.47 in the two momentum bands considered here are quite significant and very encouraging for simulation of subsequent parts of the front end.

If we follow the phase rotation channel with a charge separation system, and if we are prepared to initially transmit positive and negative particles of different momenta, then this design has the potential to significantly increase the luminosity available for the muon collider. The luminosity can be written as

$$L = \frac{N_+ N_- f}{4\pi\sigma^2}$$

where N_+ (N_-) is the number of positive (negative) particles in a bunch, f is the pulse repetition frequency, and σ is the transverse beam size at the interaction point. In the baseline design [2] two proton driver pulses are used, one for the positive particles and one for the negative particles. The timing of the two pulses on the target can be arranged so that both the positive and negative bunches traverse the phase rotation at optimum phase. However, the effective pulse repetition is reduced by a factor of 2 since only one sign is used with each proton bunch. Thus, the luminosity is proportional to the product

$$L_{\text{base}} \sim 1 \times 1 \times 0.5 = 0.5$$

For the present case, if we assume the proton driver remains the same, each of the two pulses gives the full number of positive particles and 80% of the potential number of negative particles, so the luminosity is proportional to

$$L \sim 1 \times 0.8 \times 1 = 0.8$$

Thus there is the potential for gaining a factor of 60% in luminosity with this scheme.¹

Acknowledgements

I would like to thank Juan Gallardo and the other members of the BNL group for useful discussions.

References

- [1] $\mu^+\mu^-$ Collider: a feasibility study, presented at the 1996 Snowmass Workshop, BNL-52503.
- [2] C. Ankenbrandt et al, Status of muon collider research and development and future plans, Phys. Rev. Special Topics-Accelerator and Beams, 2, 081001 (1999).
- [3] V. Balbekov, Bunch compression for a muon collider, Muon Collaboration technical note MUC-NOTE-COOL_THEORY-272, April 2003.
- [4] R. Palmer, C. Johnson & E. Keil, A cost-effective design for a neutrino factory, Muon Collaboration technical note MUC-NOTE-COOL_THEORY-67, rev. 1, November 1999.
- [5] P. Gruber et al, The study of a European neutrino factory complex, CERN-NUFACT 122, December 2002.

¹ Juan Gallardo has found that there is a phase setting that gives equal yields of positive and negative particles at the end of the channel. The positive yield is less and the negative yield is higher than the example considered here, but the luminosity gain should be similar.